The Methyl-CpG Binding Transcriptional Repressor MeCP2 Stably Associates with Nucleosomal DNA†

Simon P. Chandler, Dmitry Guschin, Nicoletta Landsberger, and Alan P. Wolffe*

Laboratory of Molecular Embryology, National Institute of Child Health and Human Development, NIH, Building 18T, Room 106, Bethesda, Maryland 20892-5431

Received January 29, 1999; Revised Manuscript Received March 17, 1999

ABSTRACT: We have investigated the interactions of the methyl-CpG binding transcriptional repressor MeCP2 with nucleosomal DNA. We find that MeCP2 forms discrete complexes with nucleosomal DNA associating with methyl-CpGs exposed in the major groove via the methyl-CpG-binding domain (MBD). In addition to the MBD, the carboxyl-terminal segment of MeCP2 facilitates binding both to naked DNA and to the nucleosome core. These observations provide a molecular mechanism by which MeCP2 can gain access to chromatin in order to target corepressor complexes that further modify chromatin structure.

DNA methylation is associated with transcriptional silencing in vertebrate genomes (*1*−*3*). Several mechanisms can contribute to silencing, and their relative importance may depend on the individual gene, cell type, and organism investigated (*4*−*6*). In mammalian tissue culture cells considerable evidence supports the selective assembly of a nuclease-resistant chromatin structure on transcriptionally repressed methylated DNA (*7*−*9*). Microinjection of methylated and unmethylated templates into *Xenopus* oocytes and mammalian tissue culture cells indicates that chromatin assembly is necessary on the Herpes Simplex Virus thymidine kinase and *Xenopus* heat shock protein 70 promoters to establish selective transcriptional repression on methylated DNA under conditions where unmethylated templates remain active (*10*−*11*). Inactive chromatin assembled on methylated DNA can also confer transcriptional silencing and nuclease resistance on adjacent unmethylated promoters (*11*, *12*). These results demonstrate that chromatin structure and function are sensitive to DNA methylation.

The most direct mechanism to alter chromatin structure on methylated DNA would be to bind repressor proteins that recognize methyl-CpG present in naked and nucleosomal DNA. These repressor proteins might wrap naked and nucleosomal DNA more stably than nucleosomal histones alone, thereby excluding both nuclease probes of chromatin structure and the transcriptional machinery. Several proteins exist that selectively recognize methylated naked DNA including MeCP1 (*13*−*15*), MeCP2 (*16*−*17*), MBD2, 3, and 4 (*18*), MDBP-2 (*19*, *20*), and histone H1 (*21*, *22*). However, although these proteins can selectively recognize naked DNA containing methylated CpG dinucleotides, with the exception of histone H1, their incorporation into a nucleosome has not been documented. The available in vivo evidence suggests that stable states of transcriptional repression dependent on DNA methylation are established and maintained within a nucleosomal infrastructure (*7*, *10*, *11*, *17*). The repressor proteins might somehow be incorporated into chromatin, but the fundamental nucleosomal repeat is retained.

Histone H1 is an intrinsic component of chromatin in the nuclei of somatic cells. It is enriched in chromatin containing methylated CpG dinucleotides (*23*) and prefers to associate with nucleosomal DNA (*24*). Although H1 can selectively associate with methylated naked DNA, the majority of somatic histone H1 variants do not discriminate between methylated and unmethylated DNA in a nucleosome in vitro (*25*, *26*). H1 is known to be a selective transcriptional repressor in vivo and in vitro (*27*−*30*); thus the potential exists for highly selective recognition of methylated DNA sequences. MDBP-2 is a proteolyzed and phosphorylated H1 variant (*19*, *20*) and, like H1 itself, might be expected to be selectively incorporated into nucleosomal DNA thereby potentially repressing transcription, since the globular domain of H1 alone retains the capacity for directing selective gene inactivation (*31*). MeCP2 appears to selectively replace histone H1 from nucleosomal templates assembled on methylated templates compared to unmethylated templates in a *Xenopus* oocyte chromatin assembly system (*17*) and is a known chromosomal protein preferentially localized to pericentric heterochromatin (*32*).

How exactly MeCP2 might be assembled into chromatin poses a significant problem. There are many impediments to trans-acting factor binding to nucleosomal DNA (*33*, *34*). An additional contributory factor to the unusual chromatin structures assembled on methylated DNA might be that the binding of methyl-CpG-binding proteins such as MeCP2 lead to the recruitment of corepressor complexes that might further modify chromatin. MeCP2 interacts with the SIN3 corepressor which in turn can recruit histone deacetylase to facilitate the modification of chromatin toward a transcriptionally repressed state (*35*, *36*). Methylated DNA is associated with hypoacetylated histones (*37*), and DNA demethylation together with inhibition of histone deacetylase can synergize to facilitate the re-expression both of silenced transgenes in transformed cell lines (*38*) and of methylated tumor sup-

† S.P.C. is the recipient of a Wellcome Trust International Prize Fellowship.

* To whom correspondence should be addressed. Tel: 301-402-2722. Fax: 301-402-1323. E-mail: awlme@helix.nih.gov.

10.1021/bi990224y CCC: $18.00
Published on Web 05/08/1999

pressor genes in human cancer cells (*39*). Together these observations provide compelling evidence of a role for chromatin in the silencing of methylated DNA.

The major evidence in conflict with the role of chromatin in transcriptional silencing derives from in vitro experiments in which MeCP1 (*14*) and MeCP2 (*17*, *40*) inhibit transcription on naked DNA added to either rat liver or HeLa nuclear extracts. Exactly how transcriptional silencing is achieved under these circumstances remains unclear. Chromatin components are present in these nuclear extracts, and although nucleosome assembly was not tested, it appears unlikely to contribute to the inhibition of transcription under the reaction conditions used. Thus multiple mechanisms may contribute to transcriptional silencing by MeCP2: those that require histones (*35*, *36*) and those that do not (*17*, *40*).

In this work we approach the issues of MeCP2 access to nucleosomal DNA. We establish that MeCP2 can associate with nucleosomal DNA, preferentially recognizing methyl-CpG dinucleotides that are exposed in the major groove of DNA as it wraps around the histone surface. Surprisingly we find that the C-terminus of MeCP2 in addition to the methyl-CpG-binding domain (MBD, ref *41*) contributes to the association of MeCP2 with both naked and nucleosomal DNA. The C-terminal domain includes the transcription repression domain (TRD, ref *17*), suggesting that multiple functions exist outside of the MBD.

MATERIALS AND METHODS

Nucleosome Reconstitution. The DNA fragments used in this study were the 218 bp *Eco*RI-*Dde*I fragment (from −79 to +137 relative to transcription start site) from the *Xenopus borealis* 5S rRNA gene which contains the intragenic promoter region (*42*, *43*), the 176 bp *Acc*I-*Dde*I fragment (from +156 to +332 relative to transcription start site) of the *Xenopus laevis* TRβA gene containing the thyroid hormone response element (TRE) (*44*), and a 222 bp *Afl*III-*Bam*HI fragment of the *Phaseolis vulgaris* β phaseolin promoter containing three phased TATA boxes (*45*). Methylation specific for the CpG dinucleotide step was carried out using *Sss*I methylase (NEB), and methylation status was checked as previously described (*26*). Nucleosome cores or histone octamers were prepared from chicken erythrocytes (*46*, *47*) and reconstituted onto radio-labeled DNA fragment by either salt exchange (gel shifts and footprints) or salt dialysis (MNase mapping) (*48*, *49*). Briefly, in the histone exchange method, a 15-fold mass excess of core particles was mixed with radio-labeled DNA at an NaCl concentration of 1 M. After a 30 min incubation at room temperature, reconstitution was achieved through slow stepwise addition of TE buffer (10 mM Tris-HCl, pH 8.0, 1 mM EDTA) until the NaCl concentration reached 50 mM. For salt dialysis reconstitution, an equal molar ratio of radio-labeled DNA fragment and purified histone octamer was mixed and NaCl added to a final concentration of 2 M. The mixture was placed in a dialysis bag and dialyzed against stepwise reductions in NaCl concentration from 2 M through 1.5, 1, 0.75, and finally 0 M in the presence of the protease inhibitor PMSF (0.2 mM).

Construction of Deletion Mutants. For MeCP2 1−467, full-length *X. laevis* MeCP2 cDNA (*35*) was subcloned into the *Eco*RI-*Hind*II sites of Pet23b (Novagen). For MeCP2 1−404, the resultant clone was then digested with *Afl*II (corresponding to amino acid position 404) and *Xho*I. These cleavages produced 3′ recessed ends which were then repaired with Klenow DNA polymerase large fragment yielding blunt ends. Religation gave deleted clones which have lost the stop codon, allowing in frame read through of the C-terminal poly His region within pET23b. The methylated DNA-binding domain (MBD) (amino acids 79−163 relative to the first methionine) and the transcriptional repression domain (TRD) (amino acids 203−305) were cloned using PCR with primers containing engineered restriction sites (*Eco*RI and *Sal*I) and ligated in frame into the corresponding sites in pRSETA (Invitrogen) and pET21a (Novagen), respectively. GST-MeCP2 was cloned in frame using a *Sma*I-*Aat*II cDNA fragment into the corresponding sites in pGex 4T-I (Pharmacia Biotech). All correct clones were expressed in BL21 DE3 pLysS cells. Cultures were grown to mid-log phase and induced with 0.4 mM IPTG for 5 h at 30 °C.

Recombinant Protein Purification. The purification of MeCP2 1−467 and MeCP2 1−404 was carried out using Ni^{2+}-NTA agarose gravity columns as in the manufacturers protocol (Novagen), except that the wash buffer was made up to a final imidazole concentration of 40 mM to avoid loss of 6 × His-tagged proteins. MeCP2 1−467 was purified by virtue of an internal poly Histidine stretch (amino acids 369−373) with the wash buffer at 60 mM imidazole. Fractions were assayed for protein content by SDS−PAGE and dialyzed versus 25 mM Tris-HCl, pH 8.0, 100 mM NaCl, 1mM β-mercaptoethanol, 2 mM $MgCl_2$, and 5% Glycerol.

The purification of GST-MeCP2 was carried out using a combination of batch and gravity flow with glutathione sepharose as in the manufacturers protocol (Pharmacia-Biotech). Elution of the bound protein was carried out with reduced glutathione. Fractions were assayed for protein content by SDS−PAGE then dialyzed against the above buffer.

Gel Shifts. Samples containing either 20 ng of naked labeled fragment or reconstituted mononucleosome (equal amounts by DNA weight) were incubated with protein in the presence of 2 mM $MgCl_2$ for 30 min at room temperature as described (*24*, *26*). Glycerol was added to the binding reactions to a final concentration of 5% (v/v), and the samples were loaded either on 0.7% agarose gels (*47*) or on 4.5%, 37.5:1 monomer/bis ratio, polyacrylamide gels containing 0.5 × TBE (1× is 90 mM Tris base/90 mM boric acid/2.5 mM EDTA). The gels were run at 200 V for 2 h at 4 °C. Gels were subsequently dried and exposed to autoradiograph film overnight at room temperature.

DNase I Footprinting. Binding reactions (100 ng DNA) were carried out as scaled up versions of the gel shift samples giving total binding and were performed as described (*24*, *26*). $MgCl_2$ was added to a final concentration of 5 mM directly before the addition of DNase I (12 ng for naked DNA samples, 30−60 ng for reconstituted samples). The DNase I reactions were carried out at room temperature for 1 min and terminated by the addition of EDTA (10 mM). Initial footprinting reactions were subsequently loaded onto a preparative gel prior to analysis by 6% denaturing polyacrylamide gel electrophoresis.

For DNase I footprints with linker histone, the H1 fraction from hydroxyl apatite chromatography of bulk chicken

erythrocyte chromatin (*46*) was bound to the reconstituted nucleosome in the presence of 50 mM NaCl. Specific marker lanes were produced by Maxam and Gilbert cleavage.

Southwestern Assay. The Southwestern procedure was as described (*16*). Extracts were made up to 20% trichloroacetic acid at 0 °C. The precipitate was collected and washed with acidic acetone before resuspending in gel loading buffer for SDS−PAGE. The proteins were then transferred to a nitrocellulose filter (BA85, Schleicher and Schuell) by electroblotting in a Bio-Rad electroblotter. Transfer was for 5 h at 35 mA at 4 °C. The transfer buffer was 25 mM Tris and 190 mM glycine. After transfer, immobilized proteins were denatured for 5 min in 6 M guanidine hydrochloride, 20 mM HEPES, pH 7.9, and 3 mM $MgCl_2$, with four successive 2-fold dilutions of the denaturing buffer with binding buffer (binding buffer is denaturing buffer minus guanidine-HCl). After two further washes with binding buffer, the filter was pre-blocked with 2% nonfat dried milk and washed again in binding buffer. ^{32}P-labeled probe (GM12, ref *41*) was added to binding buffer +0.1% Triton X-100 (about 100 000 counts min^{-1} mL^{-1}) together with nonspecific competitor DNA (20 μg/mL native *Escherichia coli* DNA, 2 μg/mL denatured *E. coli* DNA), and incubation was continued for 1 h at room temperature. The addition of Triton X-100 was found to greatly enhance the sensitivity of the assay. The filter was washed with from three to five changes (5 min each) of binding buffer supplemented with 0.01% Triton X-100. After air-drying, the filter was wrapped in Saran wrap and exposed to X-ray film. The probe in this case was a duplex DNA sequence containing 12 CpGs that were either symmetrically methylated or nonmethylated (*41*).

Micrococcal Nuclease Mapping. Mononucleosomes (80 ng of DNA) (molar ratio of histone to DNA = 1) were digested with 0.075−0.6 units of micrococcal nuclease for 5 min at room temperature as described (*24*). Incubation with linker histone and MeCP2 was as described above. Ca^{2+} was adjusted to 0.5 mM concomitant with the addition of micrococcal nuclease. Digestions were terminated with the addition of EDTA (5 mM), SDS (0.25% w/v), and proteinase K (1 mg/mL). The products of cleavage were recovered and labeled with [γ-^{32}P] ATP and T4 polynucleotide kinase. The end-labeled fragments were separated on a nondenaturing 6% polyacrylamide gel. DNA fragments of nucleosome core and chromatosome were recovered and digested with restriction enzymes to determine the boundaries of micrococcal nuclease protection. Digestions were incomplete at the concentrations of restriction enzymes used, hence some 146 and 167 bp DNA remains in the digest.

DNA−Protein Cross-Linking. DNA−protein cross-linking was performed according to the procedures of Mirzabekov and colleagues (*50*−*52*). Mononucleosomes, end-labeled to allow histone−DNA contacts to be positioned relative to one end of the molecule, were placed in a room temperature binding reaction with MeCP2 derivatives as described for the gel shifts. This incubation was followed by reaction with dimethyl sulfate (methylates purines). The methylated product is then depurinated to an aldehyde. A Schiff base is formed between the modified DNA backbone and available lysine or histidine amino acids, in the histones or MeCP2 derivatives, which can be further stabilized by reduction with sodium borohydride (*50*−*52*). Exact conditions are as follows: employing 10−25 mM dimethyl sulfate followed by incubation in 15 mM HEPES−NaOH, pH 7.4, 50 mM NaCl, 0.1 mM EDTA, and 0.1 mM PMSF at 37 °C (this gives partial depurination and subsequent cross-linking). The reaction is stopped by the addition of 25 mM $NaBH_4$ in 50 mM HEPES−NaOH, pH 7.4, on ice, followed by dialysis into 15 mM HEPES−NaOH, pH 7.4, 50 mM NaCl, and 0.1 mM EDTA.

Purification of Cross-Linked Products. The DNA−protein adducts were ethanol precipitated in the presence of 0.5% SDS. The reaction was supplemented with 0.5 mg/mL unlabeled mixed-sequence nucleosome cores isolated from chicken erythrocytes as a carrier. The protein-tagged DNA fragments were purified by KCl−SDS precipitation as described (*51*) and dissolved in loading buffer containing 9 M urea.

Two-dimensional gel electrophoresis was as described previously (*51*). The first dimension resolves the protein−DNA adducts, and then the second dimension resolves the DNA fragments. The first dimension (from left to right in the panels) requires denaturation of the protein−DNA complex by boiling in 1% SDS and 7 M urea. Resolution was achieved on a 15% polyacrylamide gel containing 0.15% SDS and 7 M urea. Resolution in the second dimension (top to bottom in the panels) follows deproteination of the complexes with a protease in, again, a 15% polyacrylamide gel containing 0.1% SDS and 7 M urea.

RESULTS AND DISCUSSION

Purification and Characterization of Recombinant MeCP2. The MeCP2 proteins used in our initial experiments are shown in Figure 1A. The purification of the three proteins is shown in Figure 1B−D. Our initial experiments made use of the GST-MeCP2 preparation (Figure 1D), and later we use the MeCP2 1−467 and MeCP2 1−404 proteins that lack the GST moiety. We have found no significant differences in the properties of GST-MeCP2 and MeCP2 1−467. A defining feature of MeCP2 is the capacity to discriminate between unmethylated and methylated DNA (*41*). To determine the DNA-binding activity of our recombinant GST-MeCP2, we electroblotted equal masses of protein from the fractions shown in Figure 1D, lanes 6 and 7, to nitrocellulose membranes before incubation with radio-labeled oligonucleotides (Southwestern assay). Probes were 40 bp in length and were either nonmethylated or methylated at 12 CpGs (GAM12, ref *41*). GST-MeCP2 interacted very weakly with the unmethylated probe (Figure 1E, lanes 1 and 2) but bound strongly to the methylated probe (lanes 3 and 4). Thus GST-MeCP2 shows the expected preference for methylated DNA (*41*). Our other recombinant MeCP2 preparations showed comparable selectivity (data not shown).

The Association of GST-MeCP2 with Nucleosomal DNA. Earlier work has shown that MeCP2 will selectively associate with a naked DNA fragment containing a single methyl-CpG dinucleotide (*41*). The MBD could protect a 12 base pair region surrounding a methyl-CpG pair with an approximate dissociation constant of 10^{-9} M (*41*). We wished to examine this interaction of MeCP2 with methyl-CpG dinucleotides in a nucleosomal context. We initially examined the interaction of GST-MeCP2 with unmethylated or methylated naked or nucleosomal DNA using agarose gel shift assays. The 215 bp *X. borealis* somatic 5S rRNA gene

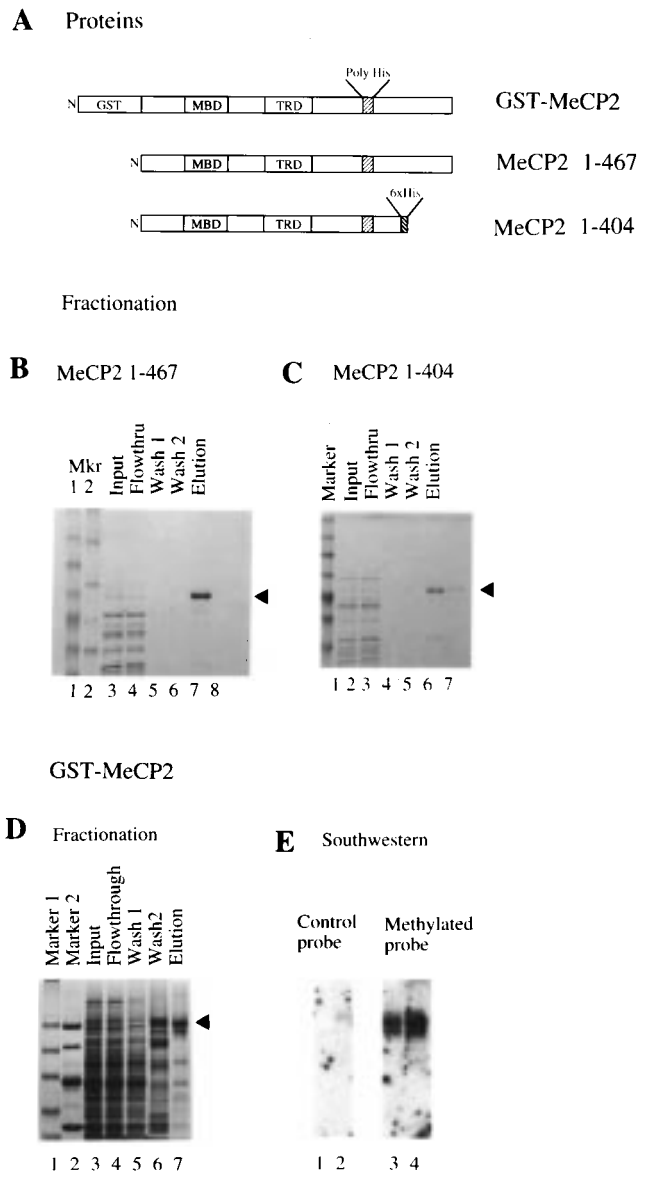

FIGURE 1: (A) Structure of GST-MeCP2 fusion and MeCP2 1−467 and MeCP2 1−404 deletion. The methylated CpG-binding domain (MBD) and the transcriptional repression domain (TRD) are shown as well as a native 11 histidine stretch (Poly His). (B, C) Purification of MeCP2 1−467 and MeCP2 1−404 by immobilized metal ion affinity chromatography. Lanes 1 and 2 (B) and lane 1 (C) are marker lanes. Lane 3 (B) and lane 2 (C) show input of cleared bacterial lysate. Lane 4 (B) and lane 3 (C) show a representative flow through fraction. Lanes 5 and 6 and lanes 4 and 5 show the washes for (B) and (C), respectively. Lanes 7 and 8 (B) and lanes 6 and 7 (C) show fractions 3 and 4 from the elution profile. Purified protein is indicated by the black arrows. (D) Purification of GST-MeCP2 by glutathione sepharose column. Lanes 1 and 2 are marker lanes. Lane 3 corresponds to the column input of cleared bacterial lysate. Lane 4 shows a representative flow through fraction. Lanes 5 and 6 correspond to washed 1 and 2. Lane 7 shows the elution from the column with the fusion protein indicated with a black arrow. (E) GST-MeCP2 has a preference for binding to methylated DNA. Southwestern assay of GST-MeCP2 (see Materials and Methods). The arrow indicates MeCP2.

fragment was either mock methylated or completely methylated at all 12 CpGs (*26*). GST-MeCP2 bound selectively to the methylated 5S DNA fragment under conditions of no detectable interaction with unmethylated DNA (see Figure 5 later; data not shown). A comparable selectivity was seen in the binding of GST-MeCP2 to methylated nucleosomal DNA compared to unmethylated nucleosomes. These experiments suggested that GST-MeCP2 can bind to methylated DNA in a nucleosome.

We next compared the DNase I cleavage patterns of nucleosomal DNA containing either MeCP2 or histone H1. Despite stable association with nucleosome cores, protection of linker DNA from micrococcal nuclease, and protein−DNA cross-linking (*24*, *26*, *53*−*56*), we have never obtained a DNase I footprint attributable to histone H1 in a mononucleosome (*24*, *26*, *56*). Our attempts to footprint histone H1 on naked unmethylated DNA (Figure 2A,B, lane 3), nucleosomal unmethylated DNA (lane 6), naked methylated DNA (lane 10), and methylated nucleosomal DNA (lane 13) likewise failed. In contrast, while GST-MeCP2 does not generate a DNase I footprint on methylated or unmethylated naked DNA (lanes 4 and 11) nor on unmethylated nucleosomal DNA (lane 7), a clear GST-MeCP2-dependent footprint is obtained on methylated nucleosomal DNA (lane 14). GST-MeCP2 protects both linker DNA and nucleosome core DNA from DNase I cleavage (Figure 2, open boxes). We conclude that MeCP2 can form a stable complex with nucleosomal DNA.

MeCP2 Protects Linker DNA from Micrococcal Nuclease Digestion. We next examined the efficiency with which micrococcal nuclease would digest the *X. borealis* 5S rRNA gene assembled into a nucleosome core in the absence of additional proteins and in the presence of histone H1 or MeCP2. Both histone H1 and MeCP2 inhibit digestion of linker DNA by micrococcal nuclease (data not shown). This result suggested that the association of MeCP2 with nucleosomal DNA will stabilize linker DNA from digestion with micrococcal nuclease. Similar results were obtained with nucleosome cores assembled on the *P. vulgaris* β-phaseolin promoter and on the *X. laevis* TRβA promoter (data not shown). For the 5S rRNA gene (Figure 3A), multiple CpG dinucleotides are distributed throughout the DNA fragment; thus the protection of linker DNA could be due either to direct association of MeCP2 with the naked linker DNA or to allosteric transitions in the nucleosome as a consequence of MeCP2 association with the nucleosome core region (*52*, *57*). Mapping the boundaries of micrococcal nuclease digestion provides one indicator of how a protein might bind to the nucleosome (*24*); however this can be subject to alternate interpretations (*58*). Thus we augmented our analysis of MeCP2 binding using protein−DNA cross-linking (*52*).

The boundaries of the DNA fragments protected from micrococcal nuclease digestion were determined by restriction endonuclease cleavage and resolution on a denaturing polyacrylamide gel (Figure 3). Incorporation of MeCP2 led to linker DNA protection similar to that of histone H1 (Figure 3B,C). For both MeCP2 and histone H1, the protection of linker DNA relative to the nucleosome core is highly asymmetric (Figure 3B,C). This result is a common feature of diverse nucleosomes reconstituted with linker histones (*24*, *52*, *58*, *59*). We next extended our analysis using protein−DNA cross-linking. Full-length MeCP2 showed extended interactions over the entire length of nucleosomal DNA, yet led to no major transitions in core-histone−DNA contacts (data not shown). To better delineate the preferred sites of contact of the methyl-CpG-binding domain of MeCP2 with the nucleosome, we made use of a C-terminal deletion mutant of MeCP2 lacking 63 amino acids, MeCP2 1−404, and the

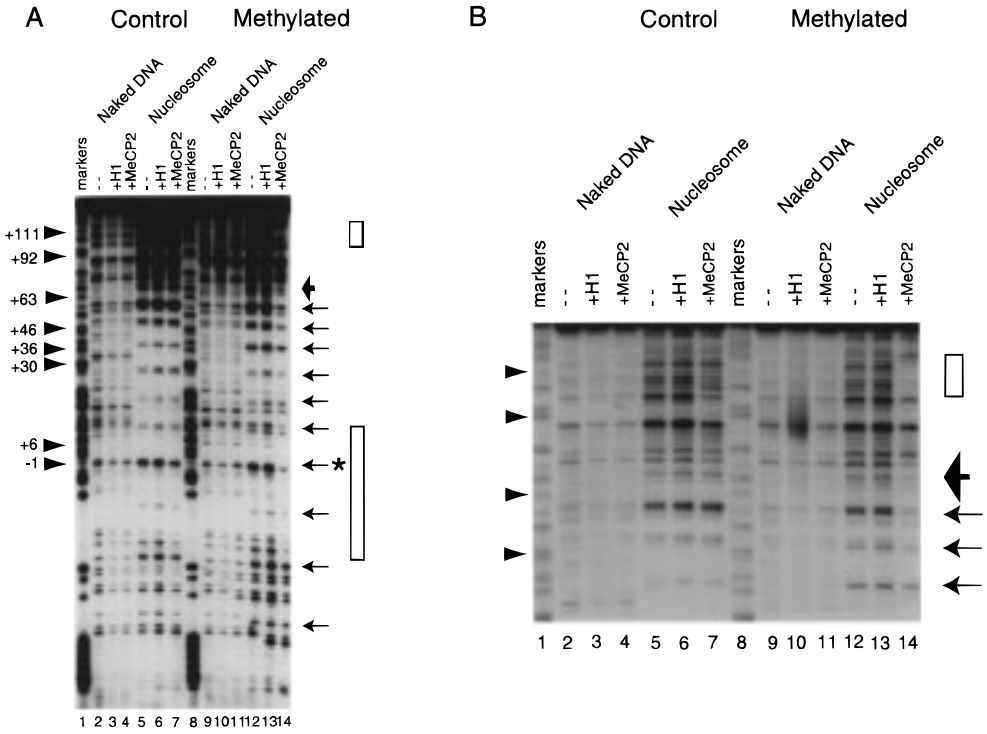

FIGURE 2: MeCP2 only shows binding specificity on the methylated 5S DNA nucleosome. (A) DNase I footprinting pattern: lanes 1−8, control DNA (unmethylated); lanes 9−14, methylated DNA. Lanes 2, 3, and 4 show DNase I cleavage products in the absence (2) and presence of H1 (3) or GST-MeCP2 (4) on control DNA; lanes 5, 6, and 7 show the digestion pattern in the absence (5) and presence of H1 (6) or GST-MeCP2 (7) on control nucleosomal DNA; lanes 9, 10, and 11 show digestion products in the absence (9) and presence of H1 (10) or GST-MeCP2 (11) on methylated DNA; lanes 12, 13, and 14 show the cleavage pattern in the absence (12) and presence of H1 (13) or GST-MeCP2 (14) on methylated nucleosome. Histone H1 is added at a molar ratio of one per nucleosome, and for GST-MeCP2, the ratio is 4:1. The positions of the CpG dinucleotide steps are indicated by black triangles on the left-hand side of the panel. The 10 bp repeat pattern indicating sites at which the minor groove is exposed in the nucleosome is shown by black arrows on the right-hand side of the panel. Also shown are boxed areas corresponding to regions protected from DNase I cleavage by MeCP2 and the dyad axis of the nucleosome core at −2, shown by an asterisk. A large black arrow denotes the nucleosomal/linker DNA boundary. (B) An enlargement of the top third of panel (A).

MBD alone. These proteins give the same micrococcal nuclease protection pattern as full-length MeCP2, yet provide more discrete DNase I footprints (see Figure 4). When mixtures of these proteins are cross-linked to 5S nucleosomes, we find that a highly asymmetric association occurs with the MBD associating preferentially with DNA proximal to the 3′ end of the 5S DNA, consistent with the micrococcal nuclease protection pattern (Figure 3D,E). We conclude that the association of the MBD with the 5S nucleosome under these conditions is highly asymmetric and that no major rearrangement of core-histone DNA contacts occurs. The asymmetric association of MeCP2 relative to the nucleosome core is similar to that of histone H1 with the 5S nucleosome (*54*, *60*, *61*); however the lack of rearrangement of core histone contacts on binding the MBD contrasts with H1 (*52*, *57*). Histone H1 has basic N- and C-terminal tail domains that can directly bind to DNA (*62*, *63*); these are absent in MeCP2.

The DNase I footprinting confirms these observations. The large horizontal arrow in Figure 2 indicates the boundary of the nucleosome core as determined by micrococcal nuclease cleavage (Figure 3). The GST-MeCP2 DNase I footprint on linker DNA includes the methyl-CpG at +111 (*42*) (Figure 2B). The linker DNA protection is consistent with the protection from micrococcal nuclease cleavage seen in the presence of GST-MeCP2 and with the protein−DNA cross-linking using the MBD (Figures 2 and 3). The small horizontal arrowheads on the right-hand side of the Figure 2 panels indicate where the minor groove of DNA within the nucleosome cores is facing out toward solution as revealed by preferential DNase I cleavage (Figure 2, compare lanes 9−11 with 12−14; see Figure 4). The major site of protection from DNase I cleavage within the nucleosome core conferred by GST-MeCP2 is over the dyad axis of this particular *X. borealis* 5S nucleosome indicated by the asterisk (Figure 2A) (−2 relative to the start site of 5S rRNA gene transcription at +1, this is derived from mapping of the micrococcal nuclease digestion boundaries to −79 and +68 as shown in Figure 3, and from earlier work; refs *24*, *57*, *60*, *61*, *64*−*67*). The positions of methyl-CpG dinucleotides in the 5S DNA sequence are indicated by the triangles on the left-hand side of the panels. Protection of the methyl-CpGs in this sequence is clearly nonuniform with GST-MeCP2 binding presumably being influenced by the nucleosomal infrastructure. We next explored this issue further.

Carboxyl-Terminal Deletions of MeCP2 Selectively Interfere with DNase I Footprint within the Nucleosome Core. Our experimental results indicate that GST-MeCP2 selectively protects some methyl-CpG dinucleotides in the nucleosome core and linker from nuclease cleavage, but not all methyl-CpG dinucleotides are protected under the conditions used (Figure 2). To address the molecular basis of selective protection of methyl-CpGs, we made use of MeCP2 1−467 lacking the GST moiety and of C-terminal truncations of MeCP2 that deleted 63 amino acids (MeCP2 1−404) or 373 amino acids (MeCP2 1−94) or that just retained the

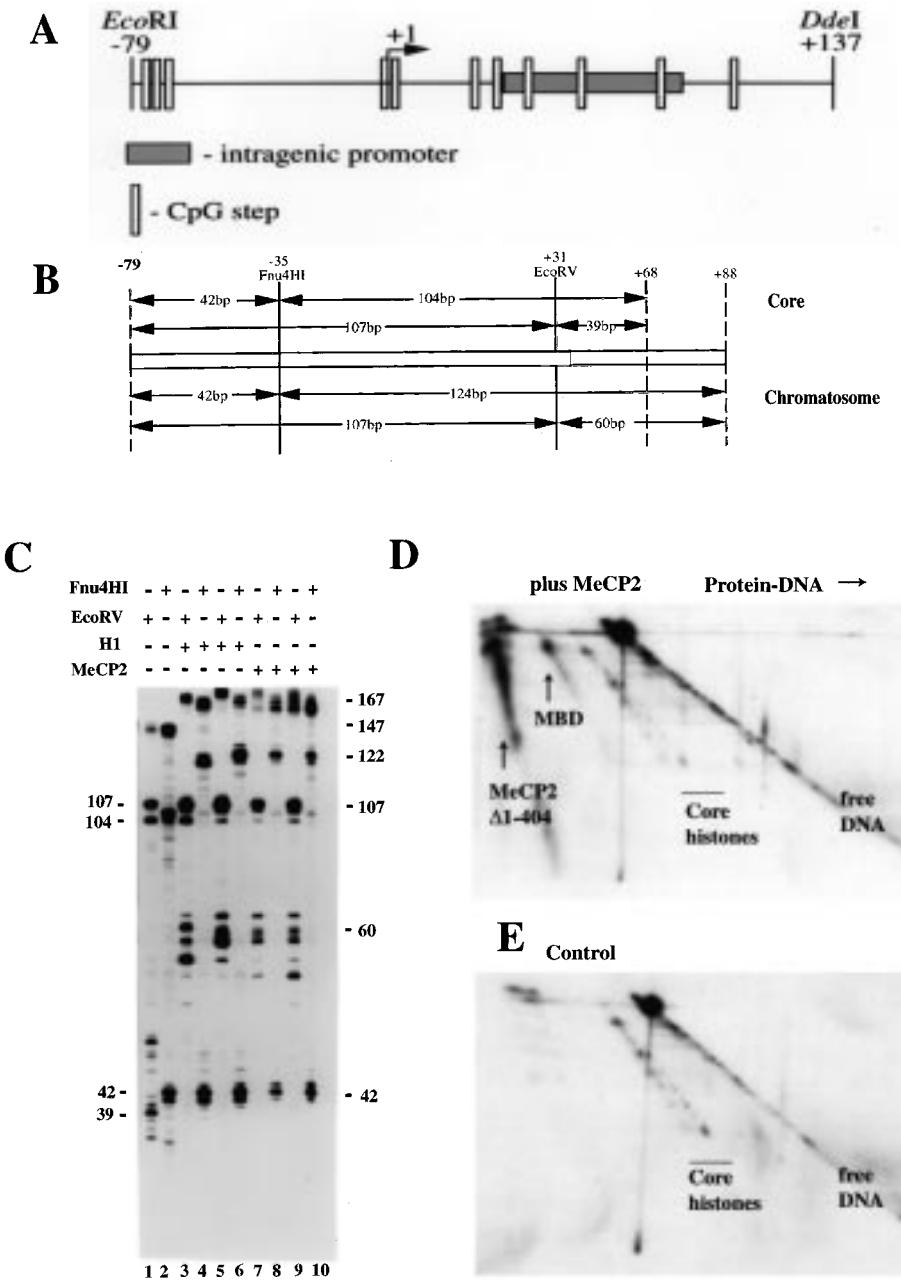

FIGURE 3: (A) Scheme of the 5S rRNA gene fragment used in these experiments showing the location of CpG dinucleotides (open boxes), the start site of transcription at +1 of gene sequence (hooked arrow), and the intragenic promoter (closed box). (B) Schematic representation of the micrococcal nuclease mapping data. The methylated 5S RNA nucleosomal and chromatosomal map. Locations of the fragments from the *Eco*RV and *Fnu*4HI digestions of the micrococcal nuclease mapping assay are shown with respect to the intragenic promoter. Micrococcal nuclease protection boundaries and restriction enzyme site positions are given with respect to the start site of transcription. (C) Asymmetric protection of the linker DNA from micrococcal nuclease by MeCP2 and H1 on the methylated 5S RNA nucleosome. Lanes 1 and 2 show methylated 5S RNA nucleosome core DNA (146 bp) cut with *Eco*RV and *Fnu*4HI, respectively. Lanes 3, 4, 5, and 6 show chromatosomal DNA (167 bp) from H1 containing nucleosomes cut with *Eco*RV (lanes 3 and 5) and *Fnu*4HI (lanes 4 and 6), respectively. Lanes 7, 8, 9, and 10 show the MeCP2−nucleosomal complex DNA (167 bp) cut with *Eco*RV (lanes 7 and 9) and *Fnu*4HI (lanes 8 and 10), respectively. (D and E) Mapping of histone DNA contacts with the top strand of the methylated 5S RNA nucleosome in the presence (D) and absence (E) of the MeCP2 derivatives: MeCP2 1−404 and the MBD. The diagonal track due to naked DNA is shown on the right-hand side of each panel (free DNA). The contacts due to core histones and MeCP2 are shown (MBD and MeCP2Δ 1−404). A 10:1 excess of MeCP2 protein derivative relative to nucleosomal DNA was used, as in the DNase I footprinting experiments shown in Figure 4B.

MBD (79−163) or transcription repression domain (TRD, 203−305) (*17*, *41*). Use of these truncated MeCP2 proteins addresses the issue of whether the methyl-CpG-binding domain alone was responsible for the nuclease protection or whether other domains might contribute either through enhancing the binding of the MBD to DNA indirectly or through direct interactions with nucleosomal DNA. Neither the TRD nor the MeCP2 1−94 proteins were able to protect DNA in the nucleosome; this result was independent of methylation status (Figure 4A). Surprisingly, deletion of the carboxyl-terminal 63 amino acids from MeCP2 to generate MeCP2 1−404 also leads to a loss of nucleosome core footprinting on reconstitution into nucleosomes. The protection of linker DNA is also severely reduced at this molar excess of MeCP2 1−404 to 5S nucleosome of 6:1 (Figure 4A, compare lane 22 and 23). The full-length MeCP2 1−467

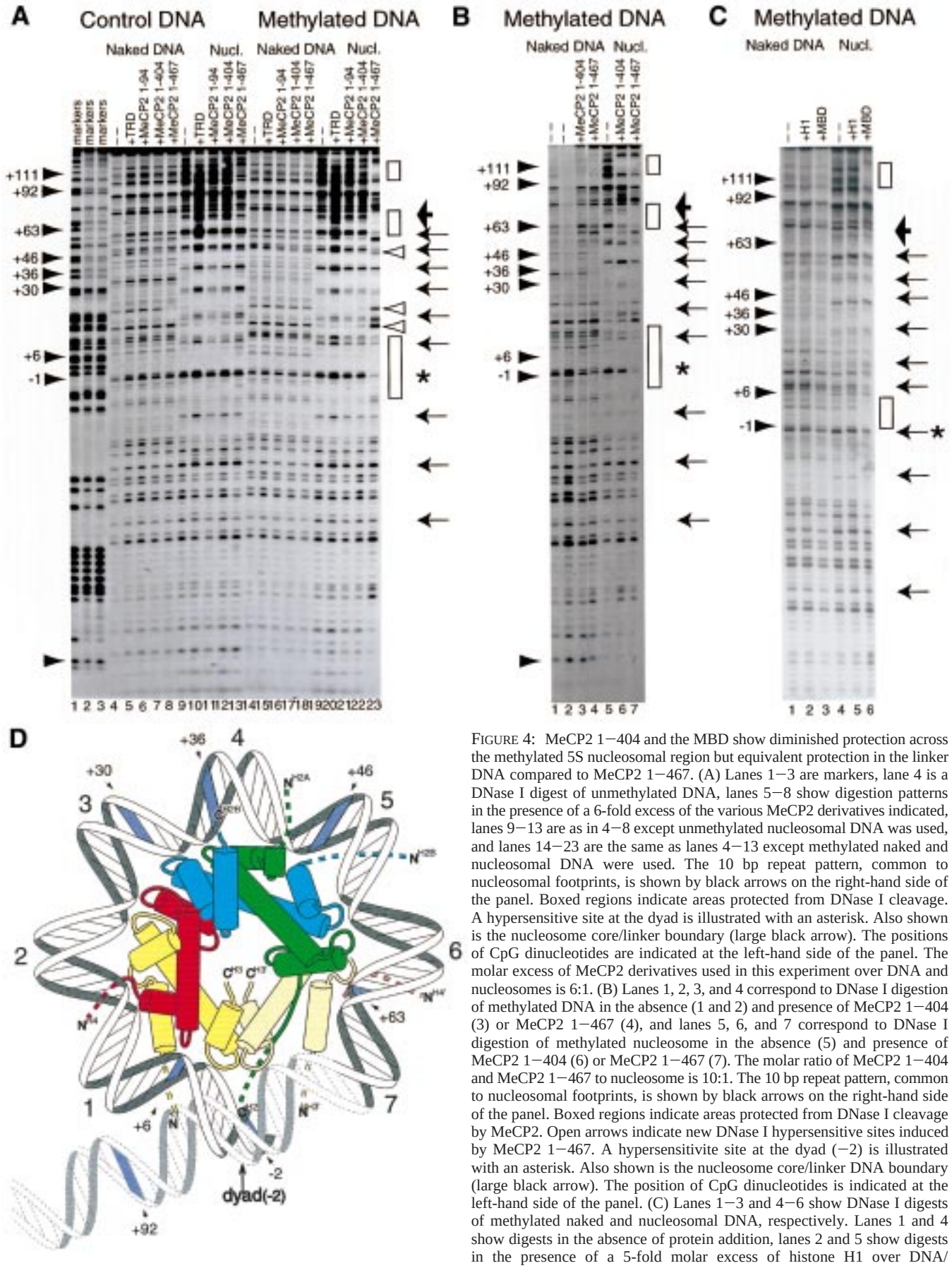

FIGURE 4: MeCP2 1−404 and the MBD show diminished protection across the methylated 5S nucleosomal region but equivalent protection in the linker DNA compared to MeCP2 1−467. (A) Lanes 1−3 are markers, lane 4 is a DNase I digest of unmethylated DNA, lanes 5−8 show digestion patterns in the presence of a 6-fold excess of the various MeCP2 derivatives indicated, lanes 9−13 are as in 4−8 except unmethylated nucleosomal DNA was used, and lanes 14−23 are the same as lanes 4−13 except methylated naked and nucleosomal DNA were used. The 10 bp repeat pattern, common to nucleosomal footprints, is shown by black arrows on the right-hand side of the panel. Boxed regions indicate areas protected from DNase I cleavage. A hypersensitive site at the dyad is illustrated with an asterisk. Also shown is the nucleosome core/linker boundary (large black arrow). The positions of CpG dinucleotides are indicated at the left-hand side of the panel. The molar excess of MeCP2 derivatives used in this experiment over DNA and nucleosomes is 6:1. (B) Lanes 1, 2, 3, and 4 correspond to DNase I digestion of methylated DNA in the absence (1 and 2) and presence of MeCP2 1−404 (3) or MeCP2 1−467 (4), and lanes 5, 6, and 7 correspond to DNase I digestion of methylated nucleosome in the absence (5) and presence of MeCP2 1−404 (6) or MeCP2 1−467 (7). The molar ratio of MeCP2 1−404 and MeCP2 1−467 to nucleosome is 10:1. The 10 bp repeat pattern, common to nucleosomal footprints, is shown by black arrows on the right-hand side of the panel. Boxed regions indicate areas protected from DNase I cleavage by MeCP2. Open arrows indicate new DNase I hypersensitive sites induced by MeCP2 1−467. A hypersensitivite site at the dyad (−2) is illustrated with an asterisk. Also shown is the nucleosome core/linker DNA boundary (large black arrow). The position of CpG dinucleotides is indicated at the left-hand side of the panel. (C) Lanes 1−3 and 4−6 show DNase I digests of methylated naked and nucleosomal DNA, respectively. Lanes 1 and 4 show digests in the absence of protein addition, lanes 2 and 5 show digests in the presence of a 5-fold molar excess of histone H1 over DNA/nucleosome, and lanes 3 and 6 show digests in the presence of a 15-fold molar excess of MBD over DNA/nucleosome. Annotation is as in A and B. (D) A model for the organization of the 5S nucleosome. The histones H3 (yellow), H4 (red), H2B (blue), and H2A (green) are shown (69−71). The position of the nucleosomal dyad reflects the predominant translational position at Figure 3 (*57*, *67*, *68*). The large numbers indicate the turns of DNA away from the dyad axis. Methyl-CpG dinucleotides are shown as blue bars and are indicated relative to the start site of transcription +1.

protects nucleosomal DNA at the dyad axis, at the boundary of the nucleosome core and in linker DNA (Figure 4A, lane 23, open boxes). A number of DNase I hypersensitive sites are also generated on addition of MeCP2 (Figure 4A, open arrows). These might indicate some local disruption of histone−DNA interactions on association of MeCP2 (*44*, *66*). An increase in the molar excess of MeCP2 1−404 to 10:1 and the resolution of the discrete nucleoprotein complex on nondenaturing polyacrylamide gels after cleavage, before deproteinization and resolution on denaturing polyacrylamide gels (*47*), allows us to show that MeCP2 1−404 protects linker DNA efficiently at +111 but shows a marked loss of protection at the nucleosome core boundary and dyad axis (Figure 4B, lane 6 open boxes). This result is consistent with the asymmetric protection from micrococcal nuclease digestion and protein−DNA cross-linking (Figure 3). We next wished to determine if the C-terminus of MeCP2 was responsible for the protection at the dyad axis or if the MBD itself could bind at multiple places in the nucleosome.

A 10:1 molar excess of the MBD to 5S nucleosome protected linker DNA at +111 but gave no detectable footprinting at the dyad axis exactly like the same excess of MeCP2 1−404 (data not shown). However a 15:1 excess of the MBD generated a complex with the 5S nucleosome that protected two discrete methyl-CpG dinucleotides at +6 and +111 (Figure 4C, lane 6, open boxes). Thus we suggest that, although the C-terminus of MeCP2 can contribute to the association of MeCP2 with 5S nucleosomes, the MBD is primarily responsible for recognition of methyl-CpGs (*41*). This result also suggests that, although the primary protection of DNA from DNase I cleavage is conferred by the MBD, the C-terminal domain of MeCP2 contributes to both the affinity of the protein for DNA and the extent of DNase I protection. For example the CpG dinucleotide at +6 is protected by MeCP2 (1−467) and by the MBD; however the pattern of protection is much more limited for the MBD than for the full-length protein. Thus either the amino acid sequences flanking the MBD contribute directly to association with DNA or they alter the MBD in order to facilitate binding.

Nucleosomal Context Influences Recognition of Methyl-CpGs. The specific nucleosomal context of the methyl-CpGs influences their recognition by the MBD. The methyl-CpG in linker DNA at +111 is preferentially occupied (Figures 3 and 4). The 5S nucleosome is modeled on the basis of the crystallographic data of Moudrianakis and colleagues (*68*−*70*), together with our own protein−DNA cross-linking data (*54*, *60*, *61*, *66*, *67*) which allows the position of the different CpGs to be predicted relative to the histone surface. Most of the methyl-CpG dinucleotides are orientated to partially face the nucleosome in the major groove; these are at −1, +30, +36, and +46 (Figure 4D). These are not strongly protected by a 6-fold molar excess of MeCP2 (Figure 4A, lane 23). Methyl-CpGs that are maximally exposed in the nucleosome core are those at +6 and +63. They are protected by full-length MeCP2 but less well by the deletion mutants (Figure 4). In addition to the methyl-CpG at +111, a second methyl-CpG lies outside the nucleosome core as defined by micrococcal nuclease at +92. There is an absence of DNase I cleavage sites in the vicinity of +92, which makes the resolution of footprinting by MeCP2 difficult to determine. An additional note of caution in the interpretation of footprinting at +92 follows from the observations that the hydroxyl radical footprint of a 5S nucleosome extends to +90 (*66*, *67*), as does the capacity to impede the binding of transcription factor TFIIIA (*71*). Thus only the DNase I footprints visible at +111 can unambiguously be explained by continued accessibility of the methyl-CpG on naked DNA. Thus known features of 5S nucleosome organization can explain the selective association of MeCP2 with particular methyl-CpGs. A prediction from this work is that the reason that methyl-CpGs within naked DNA are not protected at the same molar excesses of MeCP2 to DNA as those in the presence of the histones is the much more limited set of sites exposed in the nucleosome. This allows the limited MeCP2 in the binding reaction to saturate the exposed sites first of all.

MeCP2 Binding to the β-Phaseolin Nucleosome. Finally we wished to confirm the general features of our observations on MeCP2 binding to the 5S nucleosome using a distinct nucleosomal substrate. We made use of the *P. vulgaris* β-phaseolin promoter (*45*). This promoter contains only five methyl-CpG dinucleotides (Figure 5A). Four of these are within the nucleosome core and one lies outside (*45*). This provides a significant limitation on the choice between different CpG dinucleotides made by MeCP2 on binding to β-phaseolin compared to the 5S rRNA gene. We find that full-length MeCP2 (1−467) binds equivalently to naked and nucleosomal β-phaseolin DNA (Figure 5B, compare lanes 1−5 to lanes 10−14). Several discrete complexes are resolved in the presence of MeCP2 for both naked and nucleosomal DNA (Figure 5B), probably reflecting differential occupancy of methyl-CpG dinucleotides and their positions relative to the ends of the DNA fragments. This possibility was confirmed by DNase I footprinting analysis, which indicated similar protection of methyl-CpGs in both naked and nucleosomal DNA (Figure 5D).

A similar array of complexes are resolved in the presence of the C-terminal deletion mutant MeCP2 1−404; however binding affinity is substantially reduced relative to full-length MeCP2 for both nucleosomal and naked DNA (Figure 5C). Quantitation (not shown) indicates that full-length MeCP2 1−467 binds to methylated DNA and nucleosomes with a $K_D = 10^{-9}$ in agreement with earlier work (*41*), while the C-terminal truncated MeCP2 1−404 binds with a K_D of 8×10^{-9}. These relative values are maintained using unmethylated DNA; however the absolute values are reduced 5-fold. Earlier work (*17*, *41*) had determined the minimal requirements within MeCP2 for recognition of methyl-CpG dinucleotides, thereby defining the MBD. Our results (Figures 4 and 5) suggest that the C-terminus of MeCP2 can also facilitate association with DNA and chromatin.

CONCLUSIONS

Our results demonstrate that MeCP2 is a member of an unusual group of proteins that can bind to nucleosomal DNA without major impediment (Figures 2−5). These include the general chromatin-binding proteins histone H1 (*24*), HMG1 (*72*), HMG14/17 (*73*), and HMGI/Y (*74*, *75*) and sequence-specific DNA-binding proteins such as the glucocorticoid receptor (*76*), the thyroid hormone receptor (*44*), and HNF3 (*77*). The sequence-specific DNA-binding proteins require

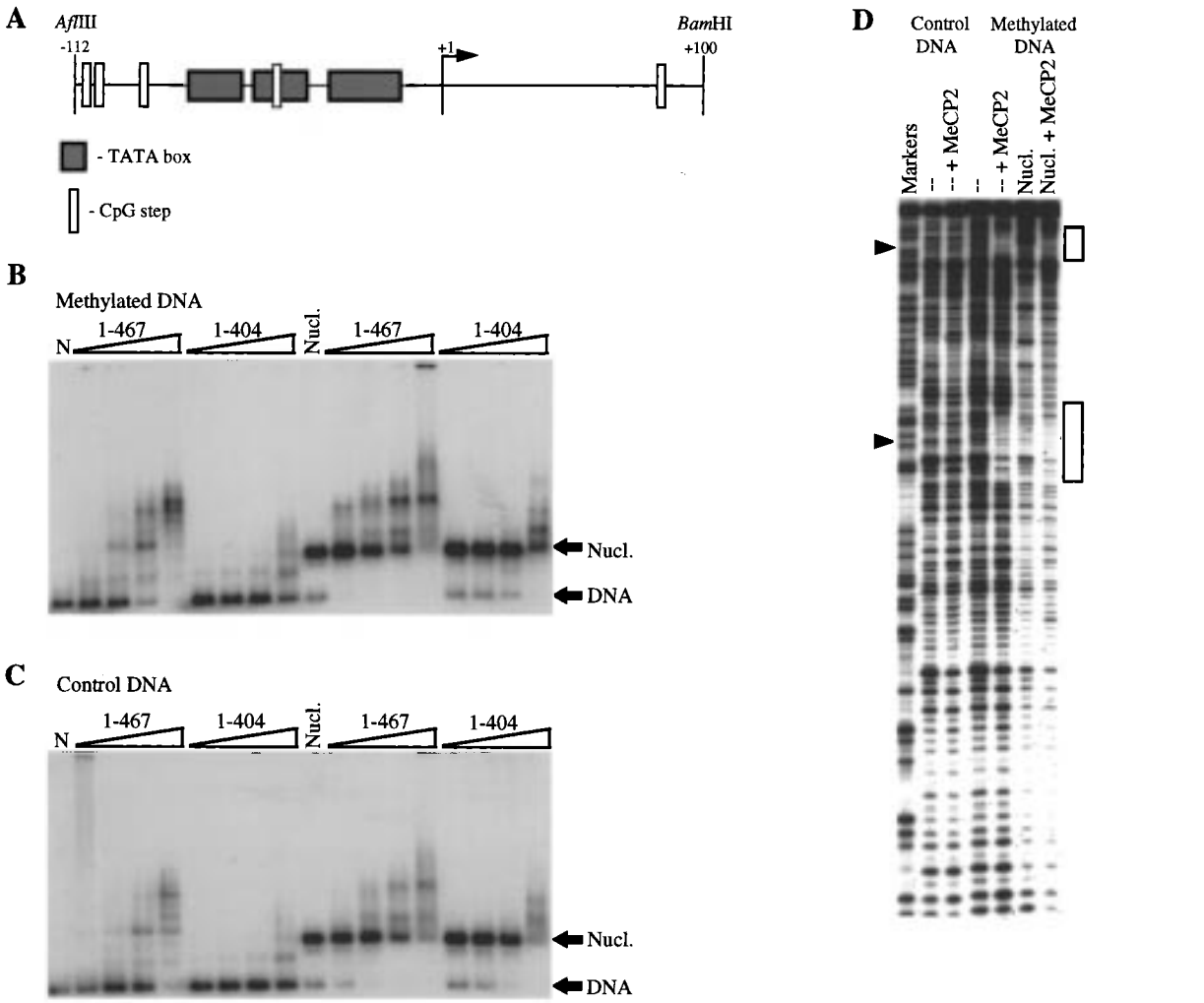

FIGURE 5: Differential affinity of MeCP2 1−467 and 1−404 on a mutant β-phaseolin promoter. (A) A schematic representation of the β-phaseolin promoter. The DNA fragment is a 219 bp *Afl*III-*Bam*HI fragment (*45*). The numbering is shown in relation to the transcriptional start site. White boxes denote the position of CpG steps within the fragment; the stippled boxes show the positions of the TATA boxes. Note that, in this mutant promoter fragment, the second TATA box is destroyed by substitution such that the second TATA box contains a CpG. (B) A gel shift comparing 1−467 and 1−404 on methylated β-phaseolin DNA and nucleosome. Lane N corresponds to naked DNA alone; "Nucl." corresponds to nucleosome alone. Subsequent lanes correspond to increasing molar ratios of DNA to protein (1:0.5, 1:1, 1:2, and 1:4). The positions of the naked DNA and nucleosomal bands are shown with black arrows. (C) A gel shift comparing 1−467 and 1−404 on the unmethylated β-phaseolin DNA and nucleosome. Annotation is as above. Lane N corresponds to naked DNA alone; "Nucl." corresponds to nucleosome alone. Subsequent lanes correspond to increasing molar ratios of DNA to protein (1:4, 1:8, 1:16, and 1:32). (D) A DNase I footprinting study of 1−467 complexed with β-phaseolin DNA and nucleosome in the presence and absence of methylation. The lanes labeled (- -) correspond to naked DNA; "Nucl." corresponds to nucleosomal DNA. The marker lane is a Maxam−Gilbert sequencing lane specific for guanine. The lanes corresponding to control and methylated DNA are shown. The positions of CpG steps resolved within the sequence are denoted by black arrowheads. The lanes containing protein are at a molar ratio of 4:1 (MeCP2/DNA) for methylated DNA and 32:1 for unmethylated DNA. Regions protected from DNase I cleavage are shown with white boxes. Note that this gel does not show all of the CpGs within the sequence.

a precise rotational positioning of their recognition elements relative to the histone surface (*66*, *78*). Similar results are obtained with MeCP2, where methyl-CpG dinucleotides that are maximally exposed toward solution are preferentially bound by MeCP2 (Figure 4). Although MeCP2 has been reported to exhibit substantial sequence selectivity in binding to DNA (*79*, *80*), we find that it has the capacity to recognize all methyl-CpGs in the 5S DNA fragment. Selectivity appears to be primarily determined by nucleosomal context. The capacity to associate with methyl-CpG in the nucleosome without the requirement for targeted nucleosome disruption ideally places MeCP2 within chromatin where it can recruit corepressor complexes to repress transcription (*35*, *36*). In this regard MeCP2 resembles the unliganded thyroid hormone receptor that can also associate with chromatin and thereby target corepressor complexes (*44*, *81*, *82*).

Earlier work established that the MBD was sufficient to recognize methylated CpG dinucleotides (*41*); however the influence of C-terminal sequences in DNA binding was not investigated. The C-terminal sequences of MeCP2 were found to contribute to transcriptional repression in vitro (*17*); however this was attributed to the presence of a transcriptional repression domain that can bind to SIN3 and histone deacetylase (*35*, *36*). Our observations indicate that the C-terminus of MeCP2 will also facilitate binding to DNA, both when naked and in the nucleosome (Figures 4 and 5). However we cannot detect binding of the TRD alone to nucleosome or DNA. The TRD might provide additional weak contacts with DNA, or it might stabilize the MRD structure itself to facilitate binding. Our data indicate that the C-terminus of MeCP2 will have multiple functions in establishing a repressive chromatin structure.

ACKNOWLEDGMENT

We thank Ms. Thuy Vo for manuscript preparation.

REFERENCES

1. Bird, A., and Tweedie, S. (1995) *Philos. Trans. R. Soc. London, Ser. B 349*, 249−253.
2. Yoder, J. A., Walsh, C. P., and Bestor, T. H. (1997) *Trends Genet. 13*, 335−340.
3. Razin, A. (1998) *EMBO J. 17*, 4905−4908.
4. Tate, P., and Bird, A. (1993) *Curr. Opin. Cell Biol. 3*, 226−231.
5. Kass, S. U., Pruss, D., and Wolffe, A. P. (1997) *Trends Genet. 13*, 444−449.
6. Nan, X., Cross, S., and Bird, A. (1998) *Norvatis Foundation Symposium 214*, 6−21.
7. Keshet, I., Lieman-Hurwitz, J., and Cedar, H. (1986) *Cell 44*, 535−543.
8. Antequera, F., Macleod, D., and Bird, A. (1989) *Cell 58*, 509−517.
9. Antequera, F., Boyes, J., and Bird, A. (1990) *Cell 62*, 503−514.
10. Buschhausen, G., Wittig, B., Graessmann, M., and Graessman, A. (1987) *Proc. Natl. Acad. Sci. U.S.A. 84*, 1177−1181.
11. Kass, S. U., Landsberger, N., and Wolffe, A. P. (1997) *Curr. Biol. 7*, 157−165.
12. Kass, S. U., Goddard, J. P., and Adams, R. L. P. (1993) *Mol. Cell Biol. 13*, 7372−7379.
13. Meehan, R. R., Lewis, J. D., McKay, S., Kleiner, E. L., and Bird, A. P. (1989) *Cell 58*, 499−507.
14. Boyes, J., and Bird, A. (1991) *Cell 64*, 1123−1134.
15. Cross, S. H., Meehan, R. R., Nan, X., and Bird, A. (1997) *Nat. Genet. 16*, 256−259.
16. Lewis, J. D., Meehan, R. R., Henzel, W. J., Maurer-Fogy, I., Jeppensen, P., Klein, G., and Bird, A. (1992) *Cell 69*, 905−914.
17. Nan, X., Campoy, J., and Bird, A. (1997) *Cell 88*, 471−481.
18. Hendrich, B., and Bird, A. (1998) *Mol. Cell Biol. 18*, 6538−6547.
19. Bruhat, A., and Jost, J. P. (1996) *Nucleic Acids Res. 24*, 1816−1821.
20. Schwarz, S., Hess, D., and Jost, J. P. (1997) *Nucleic Acids Res. 25*, 5052−5056.
21. Levine, A., Yeivin, A., Ben-Asher, E., Aloni, Y., and Razin, A. (1993) *J. Biol. Chem. 268*, 21754−21759.
22. McArthur, M., and Thomas, J. O. (1996) *EMBO J. 15*, 1705−1714.
23. Ball, D. J., Gross, D. S., and Garrard, W. T. (1983) *Proc. Natl. Acad. Sci. U.S.A. 80*, 5490−5494.
24. Hayes, J. J., and Wolffe, A. P. (1993) *Proc. Natl. Acad. Sci. U.S.A. 90*, 6415−6419.
25. Campoy, F. J., Meehan, R. R., McKay, S., Nixon, J., and Bird, A. (1995) *J. Biol. Chem. 270*, 26473−26481.
26. Nightingale, K., and Wolffe, A. P. (1995) *J. Biol. Chem. 270*, 4197−4200.
27. Bouvet, P., Dimitrov, S., and Wolffe, A. P. (1994) *Genes Dev. 8*, 1147−1159.
28. Steinbach, O. C., Wolffe, A. P., and Rupp, R. (1997) *Nature 389*, 395−399.
29. Howe, L., Itoh, T., Katagiri, C., and Ausio, J. (1998) *Biochemistry 37*, 7077−7082.
30. Sera, T., and Wolffe, A. P. (1998) *Mol. Cell. Biol. 18*, 3668−3680.
31. Vermaak, D., Steinbach, O. C., Dimitrov, S., Rupp, R. A. W., and Wolffe, A. P. (1998) *Curr. Biol. 8*, 533−536.
32. Nan, X., Tate, P., Li, E., and Bird, A. P. (1996) *Mol. Cell. Biol. 16*, 414−421.
33. Owen-Hughes, T., and Workman, J. L. (1994) *Crit. Rev. Eukaryotic Gene Expression 4*, 1−39.
34. Wolffe, A. P. (1998) *Chromatin: structure and function*, Academic Press, San Diego, CA.
35. Jones, P. L., Veenstra, G. J. C., Wade, P. A., Vermaak, D., Kass, S. U., Landsberger, N., Strouboulis, J., and Wolffe, A. P. (1998) *Nat. Genet. 19*, 187−191.
36. Nan, X., Ng, H. H., Johnson, C. A., Laherty, C. D., Turner, B. M., Eisenmann, R. N., and Bird, A. P. (1998) *Nature 393*, 386−389.
37. Eden, S., Hashimshony, T., Keshet, I., Cedar, H., and Thorne, A. W. (1998) *Nature 394*, 842.
38. Pikaart, M. J., Recillas-Targas, F., and Felsenfeld, G. (1998) *Genes Dev. 12*, 2852−2862.
39. Cameron, E. E., Bachman, K. E., Myohanen, S., Herman, J. G., and Baylin, S. B. (1999) *Nat. Genet. 21*, 103−107.
40. Meehan, R. R., Lewis, J. D., and Bird, A. P. (1992) *Nucleic Acids Res. 20*, 5085−5092.
41. Nan, X., Meehan, R. R., and Bird, A. P. (1993) *Nucleic Acids Res. 21*, 4886−4892.
42. Peterson, R. C., Doering, J. L., and Brown, D. D. (1980) *Cell 20*, 131−141.
43. Wolffe, A. P., Jordan, E., and Brown, D. D. (1986) *Cell 44*, 381−389.
44. Wong, J., Shi, Y.-B., and Wolffe, A. P. (1995) *Genes Dev. 9*, 2696−2711.
45. Li, G., Chandler, S. P., Wolffe, A. P., and Hall, T. C. (1998) *Proc. Natl. Acad. Sci. U.S.A. 95*, 4772−4777.
46. Simon, R. H., and Felsenfeld, G. (1979) *Nucleic Acids Res. 6*, 689−696.
47. Wolffe, A. P., and Hayes, J. J. (1993) *Methods Mol. Genet. 2*, 314−330.
48. Camerini-Otero, R. D., Sollner-Webb, B., and Felsenfeld, G. (1976) *Cell 8*, 333−347.
49. Tatchell, K., and van Holde, K. E. (1977) *Biochemistry 16*, 5295−5303.
50. Levina, E. S., Bavykin, S. G., Shick, V. V., and Mirzabekov, A. D. (1981) *Anal. Biochem. 110*, 93−101.
51. Mirzabekov, A. D., Bavykin, S. G., Belyavsky, A. V., Karpov, V. L., Preobrazhenskaya, O. V., Schick, V. V., and Ebralidze, K. K. (1989) *Methods Enzymol. 170*, 386−408.
52. Guschin, D., Chandler, S., and Wolffe, A. P. (1998) *Biochemistry 37*, 8629−8636.
53. Ura, K., Hayes, J. J., and Wolffe, A. P. (1995) *EMBO J. 14*, 3752−3765.
54. Pruss, D., Bartholomew, B., Persinger, J., Hayes, J., Arents, G., Moudrianakis, E. N., and Wolffe, A. P. (1996) *Science 274*, 614−617.
55. Hayes, J. J., Pruss, D., and Wolffe, A. P. (1994) *Proc. Natl. Acad. Sci. U.S.A. 91*, 7817−7821.
56. Wong, J., Li, Q., Levi, B.-Z., Shi, Y.-B., and Wolffe, A. P. (1997) *EMBO J. 16*, 7130−7145.
57. Lee, K. M., and Hayes, J. J. (1998) *Biochemistry 37*, 8622−8628.
58. An, W., Leuba, S. H., van Holde, K. E., and Zlatanova, J. (1998) *Proc. Natl. Acad. Sci. U.S.A. 95*, 3396−3401.
59. Howe, L., Iskandar, M., and Ausio, J. (1998) *J. Biol. Chem. 273*, 11625−11629.
60. Hayes, J. J. (1996) *Biochemistry 35*, 11931−11937.
61. Pruss D., Hayes, J. J., and Wolffe, A. P. (1995) *BioEssays 17*, 161−170.
62. Hill, C. S., Rimmer, J. M., Green, B. N., Finch, J. T., and Thomas, J. O. (1991) *EMBO J. 10*, 1939−1948.
63. Clark, D. J., Hill, C. S., Martin, S. R., and Thomas, J. O. (1988) *EMBO J. 7*, 69−75.
64. Wolffe, A. P., and Kurumizaka, H. (1998) *Prog. Nucleic Acid Res. Mol. Biol. 61*, 379−422.
65. Wolffe, A. P., and Hayes, J. J. (1999) *Nucleic Acids Res. 27*, 711−720.
66. Hayes, J. J., Tullius, T. D., and Wolffe, A. P. (1990) *Proc. Natl. Acad. Sci. U.S.A. 87*, 7405−7409.
67. Hayes, J. J., Clark, D. J., and Wolffe, A. P. (1991) *Proc. Natl. Acad. Sci. U.S.A. 88*, 6829−6833.
68. Arents, G., Burlingame, R. W., Wang, B. W., Love, W. E., and Moudrianakis, E. N. (1991) *Proc. Natl. Acad. Sci. U.S.A. 88*, 10148−10152.
69. Arents, G., and Moudrianakis, E. N. (1993) *Proc. Natl. Acad. Sci. U.S.A. 90*, 10489−10493.
70. Arents, G., and Moudrianakis, E. N. (1995) *Proc. Natl. Acad. Sci. U.S.A. 92*, 11170−11174.

71. Thiriet, C., and Hayes, J. J. (1998) *J. Biol. Chem. 273*, 21352−21358.
72. Nightingale, K., Dimitrov, S., Reeves, R., and Wolffe, A. P. (1996) *EMBO J. 15*, 548−561.
73. Crippa, M. P., Trieschmann, L., Alfonso, P. J., Wolffe, A. P., and Bustin, M. (1993) *EMBO J. 12*, 3855−3864.
74. Reeves, R., and Wolffe, A. P. (1996) *Biochemistry 35*, 5063−5074.
75. Bustin, M., and Reeves, R. (1996) *Prog. Nucleic Acid Res. Mol. Biol. 54*, 35−100.
76. Perlmann, T., and Wrange, O. (1988) *EMBO J. 7*, 3073−3083.
77. Cirillo, L. A., McPherson, C. E., Bossard, P., Stevens, K., Cherian, S., Shim, E. Y., Clark, K. L., Burley, S. K., and Zaret, K. S. (1998) *EMBO J. 17*, 244−254.
78. Li, Q., and Wrange, O. (1995) *Mol. Cell. Biol. 15*, 4375−4384.
79. Buhrmester, H., von Kries, J. P., and Stratling, W. H. (1995) *Biochemistry 34*, 4108−4117.
80. Weitzel, J. M., Buhrmester, H., and Stratling, W. H. (1997) *Mol. Cell. Biol. 17*, 5656−5666.
81. Laherty, C. D., Yang, W. M., Sun, J. M., Davie, J. R., Seto, E., and Eisenman, R. M. (1997) *Cell 89*, 349−356.
82. Alland, L., Muhle, R., Hou, H., Jr., Potes, J., Chin, L., Schreiber-Agus, N., and De Pinho, R. A. (1997) *Nature 387*, 49−55.

BI990224Y